RESEARCH ARTICLE

Glenn Thompson · Stephen R. McNutt · Guy Tytgat

# Three distinct regimes of volcanic tremor associated with the eruption of Shishaldin Volcano, Alaska 1999

**Abstract** Tremor signals associated with the eruption of Shishaldin Volcano on 19 and 23 April 1999 were the strongest recorded anywhere in the Aleutian Arc by the Alaska Volcano Observatory (AVO) in its 10-year history. Reduced displacements ($D_R$) reached 23 cm$^2$ on 19 April and 43 cm$^2$ on 23 April. During the activity, $D_R$ and spectral data with a frequency resolution of 0.1 Hz were computed and put on the World Wide Web every 10 min. These data are analyzed here. The general temporal patterns of seismicity of these eruption events were similar, but the eruptions and their effects quite different. The 19 April event is known to have culminated in a sub-Plinian phase, which ejected ash to an altitude of 16 km. Despite higher amplitudes and the largest hotspot from satellite data, the 23 April event produced little ash reaching only 6 km altitude. For several hours prior to the sub-Plinian phase on 19 April, tremor with a peak frequency of 1.3 Hz intensified. During the sub-Plinian phase the peak frequency increased to 4–8 Hz. However, in 15 h after the eruption, three episodes of stronger tremor occurred with a lower 1.0-Hz peak, alternating with weaker tremor with a 1.3-Hz peak. These transitions correspond to $D_R$=~8 cm$^2$. Although these strong tremor episodes produced higher $D_R$ levels than the sub-Plinian phase, data from a pressure sensor show that only strong Strombolian explosions occurred. The suite of observations suggests three distinct tremor regimes that may correspond to slug flow, bubbly flow, and sustained strong eruptions, or a cyclic change in source parameters (e.g., geometry, sound speed, or ascent rate). This behavior occurred at Shishaldin only during the April 1999 sequence, and we are not aware of similar behavior at other volcanoes.

**Keywords** Alaska · Shishaldin Volcano · Volcanic tremor

S.R. McNutt (✉) · G. Tytgat
Alaska Volcano Observatory, Geophysical Institute,
University of Alaska Fairbanks, P.O. Box 757320, Fairbanks,
AK 99775-7320, USA
e-mail: steve@giseis.alaska.edu

G. Thompson
Montserrat Volcano Observatory, Mongo Hill, Montserrat,
West Indies

## Introduction

Shishaldin is the most active volcano on Unimak Island, and the second most active in the Alaska/Aleutian Arc (Miller et al. 1998). A new seismic network was installed by the Alaska Volcano Observatory (AVO) in July 1997 (Fig. 1), consisting of six short-period seismic stations; six additional stations were installed at nearby Westdahl Volcano (60 km WSW) in July 1998. A single pressure sensor is co-located with seismic station SSLN (Fig. 1). These stations permit the first observations of seismic and acoustic activity associated with an eruption of Shishaldin. In this paper, we give an overview of volcanic tremor, focusing on data associated with the initial stages of the explosive eruption on April 1999.

Seismic and thermal unrest were noted in January–February 1999 (Nye et al. 2002, this volume), and intensified in March when a vigorous earthquake swarm occurred 15 km to the west (Moran et al. 2002, this volume). On 7 and 14 April seismicity increases may have been associated with small eruptions. Strombolian lava fountaining was observed on 17 April (Nye et al. 2002, this volume), and a sub-Plinian phase occurred on 19 April lasting 50–80 min, followed by three additional strong Strombolian phases. On 23 April, another eruption event occurred, producing a large thermal anomaly (Dehn et al. 2002, this volume) but only a weak ash plume. Mild eruptive activity continued until May 1999.

Volcanic tremor, a continuous vibration of the ground, was observed before, during, and after the 1999 eruption of Shishaldin. Tremor is a ubiquitous signal at active

**Shishaldin Volcano Seismic Network**
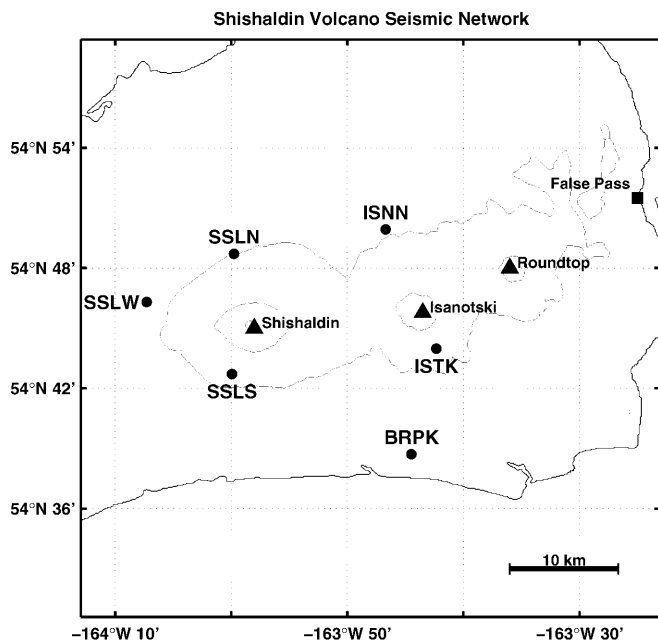


**Fig. 1** Map of volcanoes (*triangles*), seismic stations (*circles*), and settlements (*squares*) on Unimak Island, Alaska. All stations have 1-Hz vertical geophones except SSLS, which has 2-Hz 3-component geophones. Station SSLN also has a pressure sensor. The Westdahl network (not shown) is 47 to 63 km to the southwest from Shishaldin's summit. Contour interval 3000 ft (914 m)

volcanoes and has been observed at over 160 volcanoes worldwide (McNutt 1994b). Shishaldin tremor was first observed at very low levels on 9 January 1999, and was strong enough to be definite on 9 February 1999. The tremor was more or less stationary from February to April, gradually increasing in amplitude. Tremor increased abruptly on 7 April to levels comparable to those associated with eruptions elsewhere (reduced displacement $D_R$=8 cm$^2$), however, no confirmation of eruption could be obtained due to poor weather. Tremor then returned to lower levels, and began to increase again on 15 April. Visual confirmation of Strombolian activity was obtained on 17 April, when the tremor level was $D_R$=2–3 cm$^2$, again similar to values observed elsewhere in association with minor eruptions. Examples of tremor seismograms are shown in Fig. 2.

The VEI =3 eruptions that began on 19 and 23 April had similar temporal patterns of seismicity, with slow tremor buildups and abrupt ends, but the former produced a significantly larger ash column and the only significant tephra deposit. During the 23 April event, tremor was strong enough to be recorded on the Westdahl, Akutan and Pavlof Volcano seismic networks, the latter two each about 160 km from Shishaldin. Reduced displacement plots (Fig. 3) and spectrograms (Fig. 4) show three distinct regimes of tremor suggestive of different styles of eruptive activity from 19 to 23 April. Further, the pressure sensor data also show different behavior for the three regimes. Detailed analyses of the 19 April tremor sequence are the main focus of this paper.

## Data

AVO operates a network of six short-period seismic stations on Shishaldin. All stations have T=1 s vertical component geophones (Mark Products L-4C) except SSLS, which has T=0.5 s, 3-component geophones (Mark Products L-22). All data are FM-radio telemetered to the nearby towns of Cold Bay and King Cove, then transmitted by telephone lines to AVO in Fairbanks. There the analog signals are digitized at 12 bits and recorded continuously at a sample rate of 100 Hz on several different computer systems. A pressure sensor is operated at one site, SSLN (Fig. 1). The data are telemetered and recorded in the same manner as the seismic data. Times given in this paper are UTC (Universal Time Coordinated) and AST (Alaska Standard Time) where AST =UTC –8 h.

Shishaldin is one of 23 volcanoes that are monitored in near-real-time using the IceWeb system (Benoit et al 1998; Thompson et al., in preparation). This system computes frequency spectrograms and reduced displacement ($D_R$) for three to six stations at each volcano, then uploads plots of these data to the World Wide Web every 10 min. Spectra are computed for 10-s windows of data with 5-s overlap. The individual spectra are then replotted as spectrograms of 10 min duration. Plots have a frequency resolution of 0.1 Hz. $D_R$ is an absolute measure of tremor amplitude (see the Appendix), equal to the maximum sustained rms ground displacement corrected for geometrical spreading (Aki and Koyanagi 1981; Fehler 1983), and is related to ash column height (McNutt 1994a). IceWeb $D_R$ plots show one data point every 10 min using a different color for each station. The vertical scale of the web plots is logarithmic to help identify eruption onsets, for which the signals are often observed to increase exponentially, thus appearing as a straight line on the plots. For this paper, data were replotted with a linear vertical scale (see Fig. 3). Both spectral and $D_R$ data are archived and tools exist for creating plots of these data for any time period (e.g., Figs. 4 and 5). The pressure data were not automatically processed on the Web, but, instead, selected portions of data were analyzed to help answer questions posed during this study. A full treatment of the pressure data will be the topic of a future study (Caplan-Auerbach and McNutt, submitted).

## Analyses and results

Spectrograms and $D_R$ plots were available for seismic data for the entire precursory and eruptive episodes. Therefore, we examined the co-eruptive data in detail and performed additional analyses on selected portions. Spectrograms (Fig. 4b) hint at a change in the dominant frequency of the tremor signal to a lower frequency after the 80-min-long sub-Plinian phase on 19 April. When these spectral data were analyzed in more detail it was clear that there were several spectral peaks that varied in
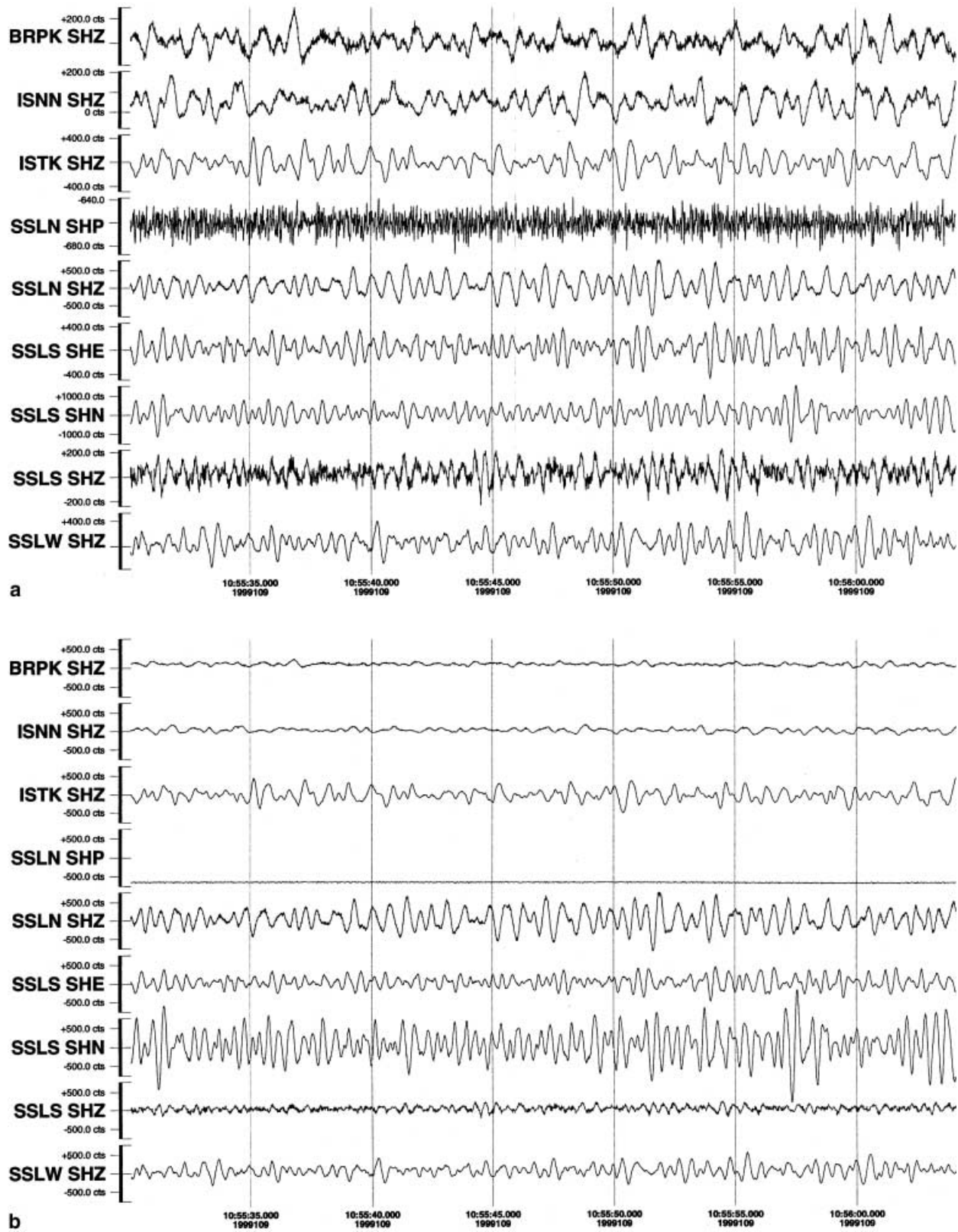
**Fig. 2a, b** Examples of seismograms for Shishaldin volcanic tremor on 28 March 1999. Thirty-five (35) seconds of data are shown. **a** Normalized amplitudes. **b** True relative amplitudes. Station locations are shown in Fig. 1; SSLN SHP is a pressure sensor.
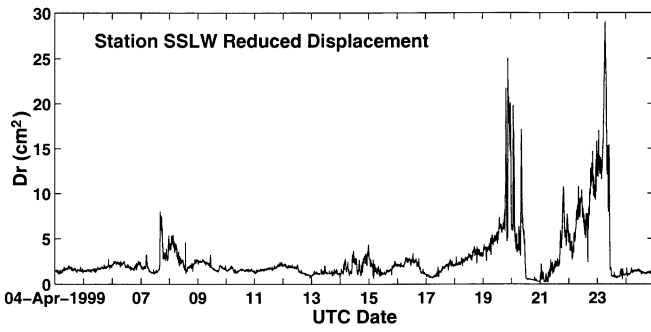
538



**Fig. 3** Reduced displacement ($D_R$) for 4–24 April 1999 at Shishaldin Volcano. Data are from station SSLW. $D_R$ has units of cm$^2$ and is an absolute measure of tremor amplitude. The surface wave formulation was used for this plot (see the Appendix). Strong $D_R$ accompanied eruptions on 19 and 23 April. AST =UTC –8 h

their relative amplitudes, making it difficult to evaluate if the suspected drop in frequency was real. However, the spectrograms do suggest that the broad spectral energy was shifted to a lower frequency, and the best way to investigate this is to look for changes in the mean frequency of the signal.

Mean frequency (fmean) data were computed for three stations – SSLW (10.1 km), ISTK (17 km), and ISNN (14.8 km)- for a 36-h period beginning at 00:00 UTC on 19 April (16:00 h AST 18 April). These data are remarkably well correlated (Fig. 6). The fmean on SSLW is ~ 10% greater than that on ISTK and ~ 20% greater than that on ISNN, perhaps because of path or site effects, but the patterns are almost identical and clearly reflect a strong source effect for the tremor. These data show that rather than a single shift in tremor frequency after the sub-Plinian phase on 19 April, there were in fact several shifts over the following 16 h. Data from outside the 0.5–5-Hz frequency band were excluded

**Fig. 4a–c** Spectrograms for the three eruptive sequences on 7 April 19 April and 23 April. *Red* for strong signal, *blue* for weak signal, *yellow* for intermediate values. Tremor frequencies were dominantly 1–2.5 Hz. **a** Abrupt onset, gradual fade. $D_R$ levels indicate VEI=2 eruption. No corresponding deposits have been identified. **b** Gradual onset marked by Strombolian activity. Climaxed in a VEI=3 eruption, which sent ash up to an altitude of ~16 km. Three pulses of high-amplitude tremor after initial phase. Abrupt end. **c** More rapid onset. Produced the strongest tremor of the Shishaldin unrest and the largest observed thermal anomaly, but little ash. Two pulses of strong tremor occurred after the main phase. Abrupt end. For all plots, AST=UTC –8 h
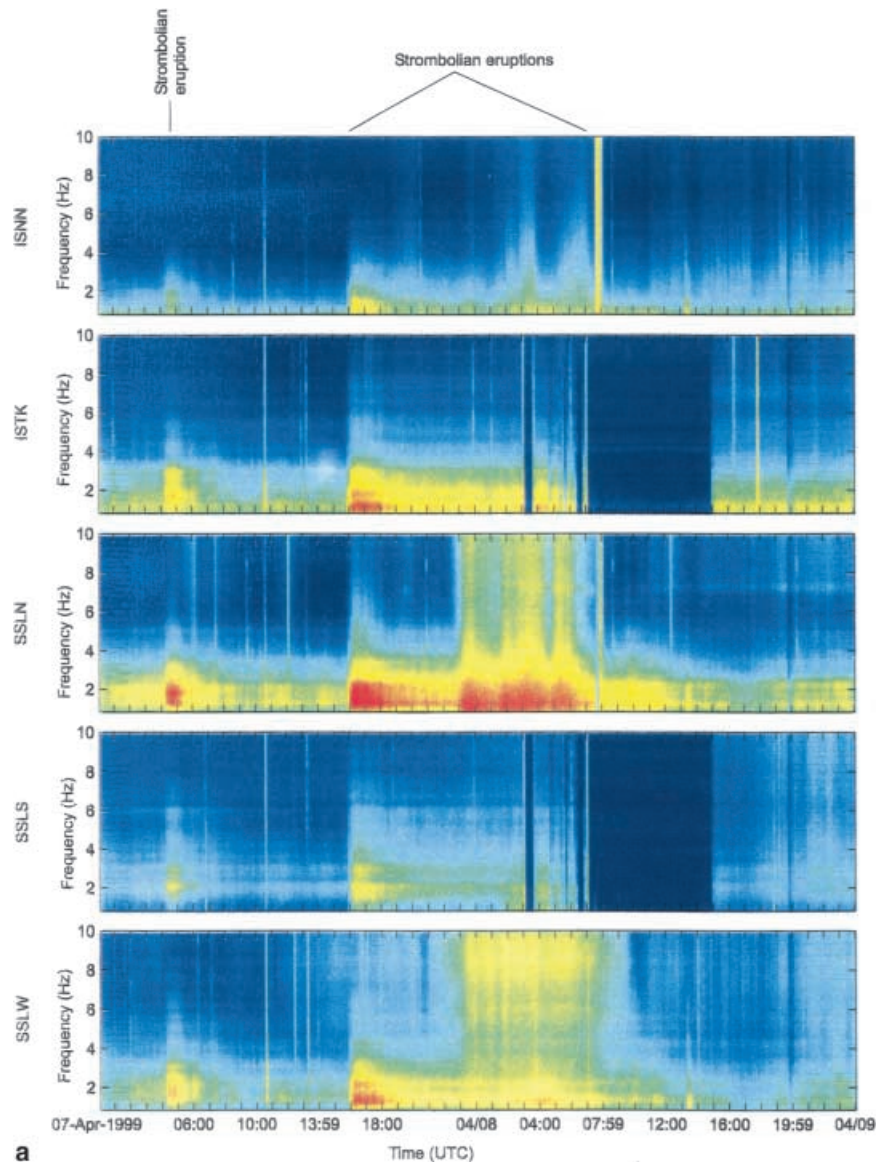
from this study to reduce non-tremor signal from ocean microseisms and wind. Station SSLS stopped transmitting data during the sub-Plinian phase on 19 April; it was probably struck by lightning from the ash cloud. Station SSLN was saturated (clipped) and so is excluded from our analysis. These five stations were the only stations on the IceWeb system and so are the only stations for which the continuous spectral data exist.

These fmean signals were stacked to increase the signal-to-noise ratio and to enhance the source effect, and plotted against a stacked reduced displacement trace for the same three stations (Fig. 5). Four tremor signals were identified from comparison of these fmean and $D_R$ traces and are henceforth referred to as Strombolian, sub-Plinian, vigorous Strombolian, and background tremor respectively (see Table 1). The term "vigorous Strombolian" is a relative term used only in this paper, for reasons explained below. Strombolian tremor occurred between 00:00–19:00 h UTC on 19 April (16:00 h 18 April to 11:00 h AST 19 April) and was characterized by slowly increasing $D_R$ <8 cm², and fmean ~ 2.0 Hz. Sub-Plinian tremor lasted from ~19:30–20:20 h UTC (11:30–12:20 h AST) and was marked by a broadband (hence the relatively high fmean ~ 2.4 Hz) tremor signal with maximum $D_R$=23 cm². Between 21:00 h UTC 19 April (13:00 h AST) and 12:00 h UTC the following day (04:00 h AST 20 April) there then followed several cycles of alternating vigorous Strombolian tremor ($D_R$>20 cm², fmean ~1.7 Hz) and background tremor ($D_R$ <8 cm², fmean ~2.0 Hz). Tremor on 23 April was the strongest observed by AVO in its 10-year history, and reached $D_R$=43 cm². (Data for station SSLW, shown in Fig. 3, were partially saturated on 23 April. This is the reason the plotted value in the figure differs from that cited in the text.)
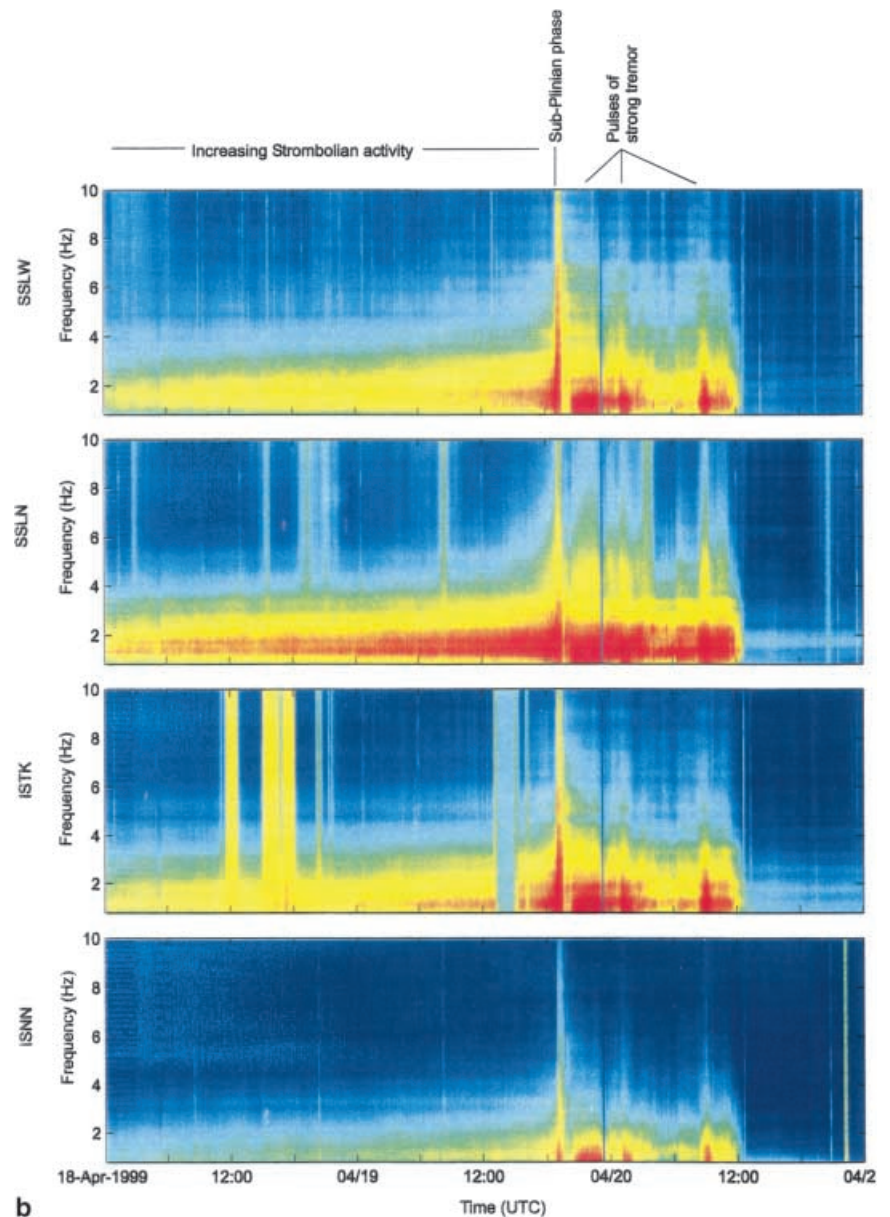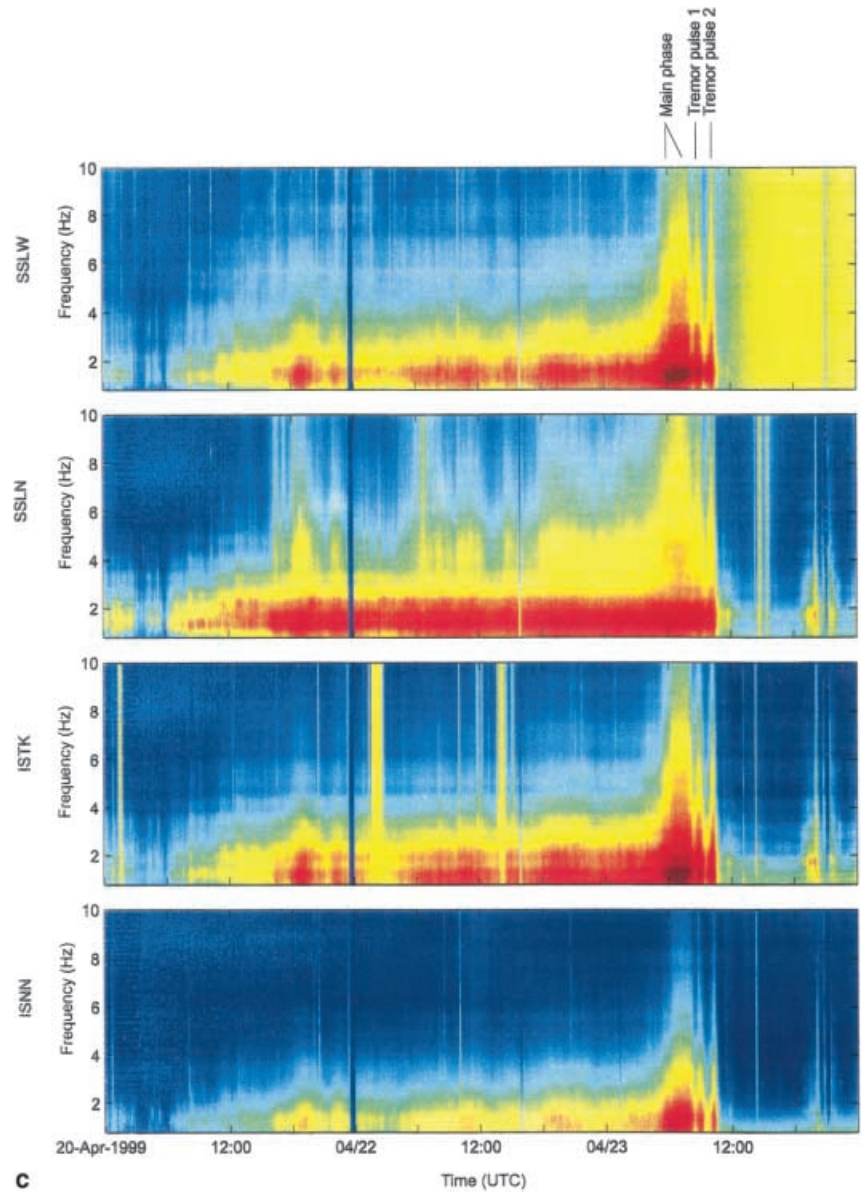
**Fig. 4a–c** (continued)



b

**Fig. 4a–c** (continued)



c

Time (UTC)

$D_R$ is a standard method of normalizing volcanic tremor recorded at varying distance from a volcano to a common scale. Table 2 shows $D_R$ values computed using both the surface wave and body wave formulations (Aki and Koyanagi 1981; Fehler 1983). For details of these calculations, see Appendix 1. We chose the surface wave formulation as the long-term default; therefore, the plots shown in this paper, and in Nye et al. (2002, this volume) and Schneider et al. (1999) all use this default. However,

**Fig. 5** Mean frequency (*top*) and reduced displacement (*bottom*) versus time (AST=UTC –8 h) using stacked data from stations SSLW, ISTK, and ISNN. The sub-Plinian eruption is characterized by a high-amplitude signal with a high mean frequency. Prior to this is a gradually increasing signal with constant mean frequency. After the eruption, bands of high-amplitude, low-mean-frequency signal alternate with bands of low-amplitude, higher-mean-frequency signal
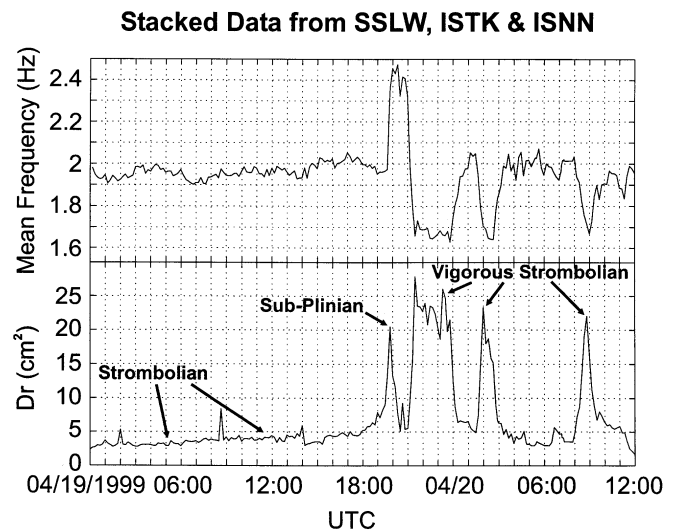


**Stacked Data from SSLW, ISTK & ISNN**

**Fig. 6** Mean frequency of the tremor between 0.5–5 Hz plotted for three stations against time [UTC; local time (AST) is UTC –8]. These traces have a high correlation coefficient, suggesting source effects. Note the relatively steady frequencies from 00:00 to 19:40 h. The sub-Plinian eruption corresponds to a high-frequency burst beginning at 19:40 h. Immediately after this eruption the mean frequency is 10% lower than that observed before the eruption until 00:00 h. The frequency then returns to background, followed by two additional low-frequency episodes beginning at 02:00 and 08:30 h
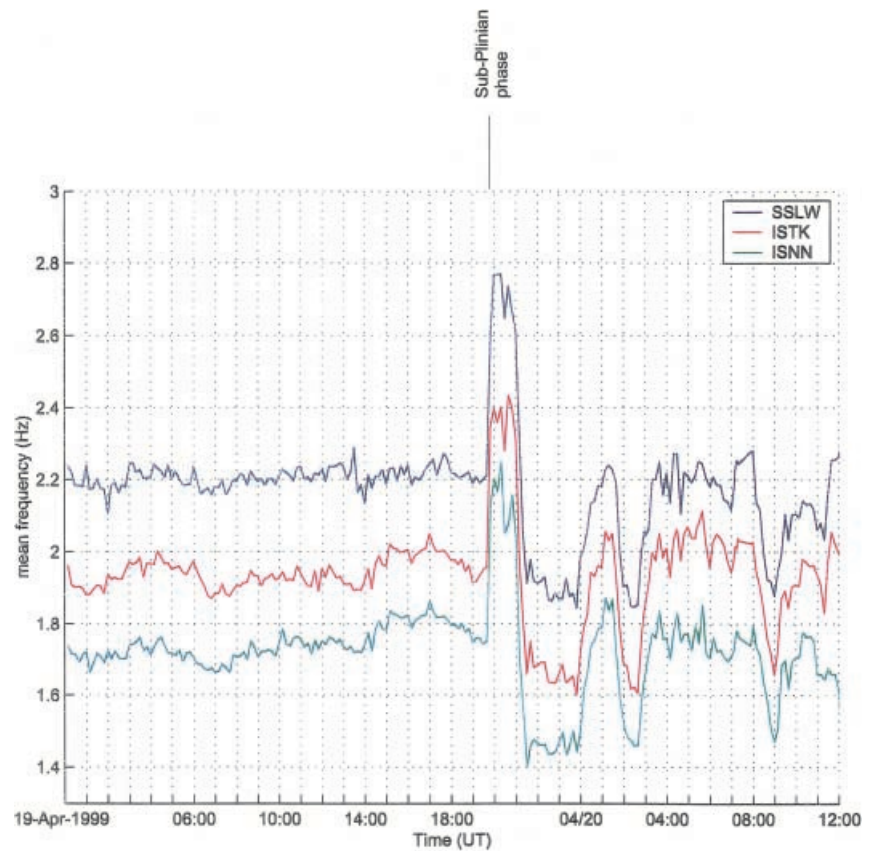


**Table 1** Parameters of volcanic tremor and explosions at Shishaldin, January to April 1999

| Date | Phase | $D_R$[a] (cm$^2$) | Freq. (Hz) | Erupted volume ($\times 10^6$ m$^3$) | Explosion rate, no. per 3 min, stn. SSLN-P | Explosion amplitude, counts, stn. SSLN-P |
|---|---|---|---|---|---|---|
| Jan.–6 April | Background | 0.5–2 | 1–2.5 | Negligible | 0 | – |
| 7 April | Strombolian | 16 | 1–2.5 | Not known | 0 | – |
| 8–19 April | Strombolian | 0.5–5 | 1–2.5 | Minor | 0 | – |
| 19 April | Sub-Plinian | 46 | 3.5–8.4 | 14 | 1–6 | 100 |
| 19 April | Vigorous Strombolian I | 48 | 0.9–1.2 | Minor | 48 | 120 |
| 19 April | Background I | 7 | 1–2.5 | Negligible | 0 | 40 |
| 19 April | Vigorous Strombolian II | 40 | 1.2 | Minor | 26 | 130 |
| 19 April | Background II | 5 | 1–2.5 | Negligible | 0 | 50 |
| 19 April | Vigorous Strombolian III | 36 | 0.8–1.2 | Minor | 23 | 90 |
| 19 April | Background III | <5 | 1.6 | Negligible | 1 | 60 |
| 23 April | Vigorous Strombolian | 89 | 1.2 | Minor[b] | 30 | 1,000 |

[a] Preferred values for reduced displacement ($D_R$) shown here; see text and Table 2

[b] A large hot spot was observed in satellite data, but no discrete deposit was found

preliminary analyses of waveforms on three-component data show both body wave and surface wave contributions. Hence, our preferred values are averages of the two and are shown in Tables 1 and 2. We have retained the default values for the plots to avoid confusion with the original data. Conclusions, however, are based on consideration of all data including the preferred values.

Based on frequency and $D_R$, Strombolian tremor before 19 April and low-amplitude tremor after the sub-Plinian eruption may be the same. This conclusion is

supported by further spectral analyses. Spectral data for each tremor signal were stacked to produce representative (smoothed) spectra (Fig. 7a). Spectral ratios were also examined, using the Strombolian tremor as a reference spectrum (Fig. 7b). Spectra for both the Strombolian and low amplitude tremor show a main peak around 1.3 Hz and the spectral ratio is close to 1 at all frequencies. The high amplitude tremor signal has a much lower frequency main peak from 0.9–1.0 Hz and is relatively narrow-band. The sub-Plinian tremor signal is relatively

542

**Table 2** Shishaldin Volcanic tremor reduced displacement ($D_R$) April 1999

| Date | Phase | $D_R$ using surface waves (cm$^2$) | $D_R$ using body waves (cm$^2$) | Preferred mean $D_R$ (cm$^2$) |
|---|---|---|---|---|
| 7 April | Strombolian | 8 | 24 | 16 |
| 19 April | Sub-Plinian | 23 | 69 | 46 |
| 23 April | Vigorous Strombolian | 43 | 134 | 89 |

**Fig. 7 a** Smoothed spectra for each tremor signal. **b** Spectral ratios for strong tremor relative to Strombolian tremor for the 19 April sequence. During the sub-Plinian eruption, dominant frequencies were 3.5–8.4 Hz, with a minor peak at 0.9–1.0 Hz. During the three later episodes of high-amplitude tremor the 0.9–1.0-Hz peak was dominant and a broad secondary peak is evident between 4.5–6.3 Hz. Low-amplitude tremor is essentially identical to Strombolian tremor as indicated by the flat spectrum. Data are from station ISNN
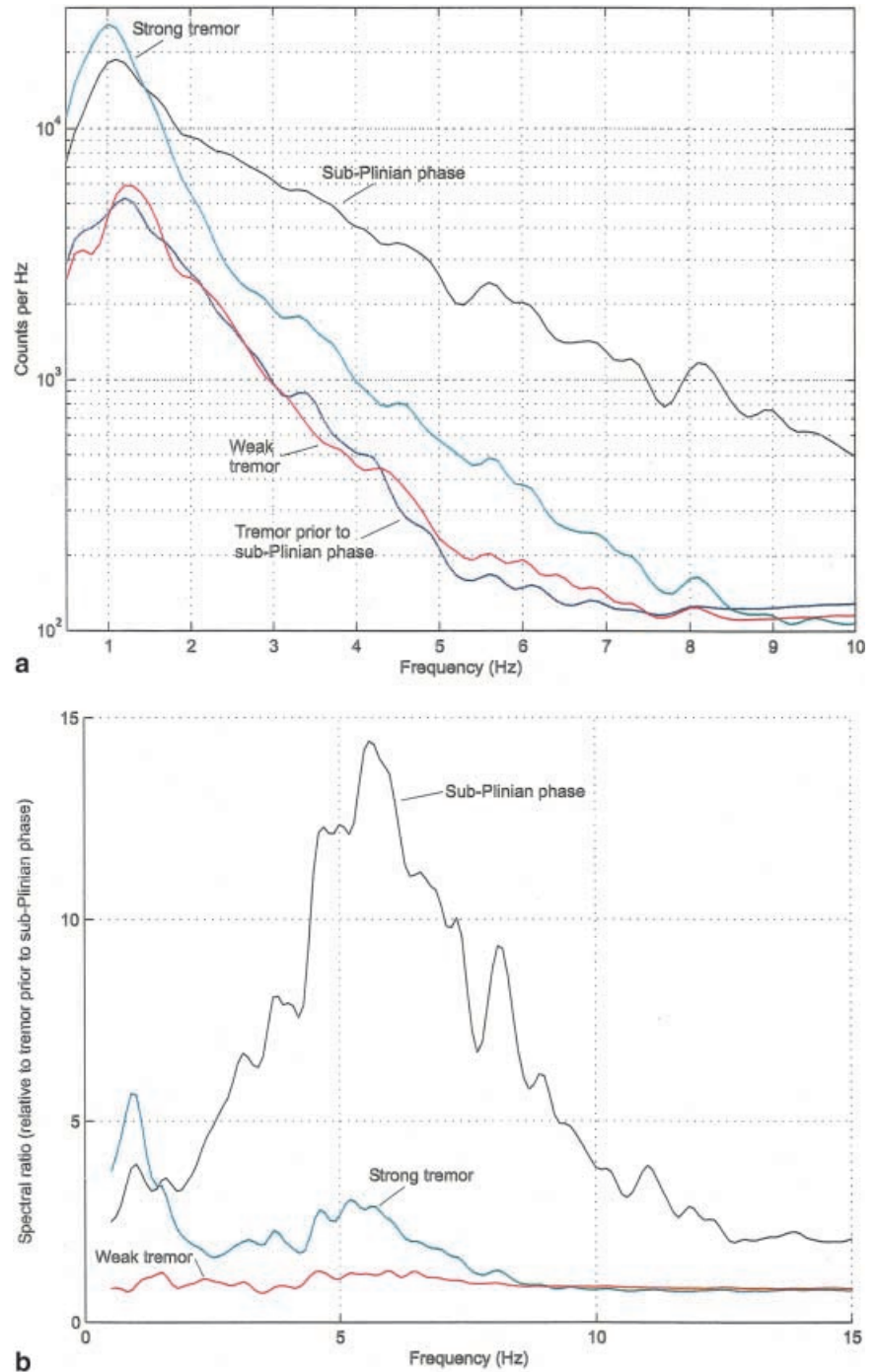
Fig. 8a–f Pressure time series and spectrograms from station SSLN pressure sensor. a 19 April at 18:00 h UTC (10:00 h AST); Strombolian activity. b 19 April at 19:50 h UTC (11:50 h AST); sub-Plinian phase. c 19 April at 23:05 h UTC (15:05 h AST); vigorous Strombolian explosions. d 20 April at 01:00 h UTC (17:00 h AST 19 April); background Strombolian. e 20 April at 01:47 h UTC (17:47 h AST 19 April); vigorous Strombolian. f 23 April at 10:01 h UTC (02:01 h AST); strongest observed Strombolian explosions
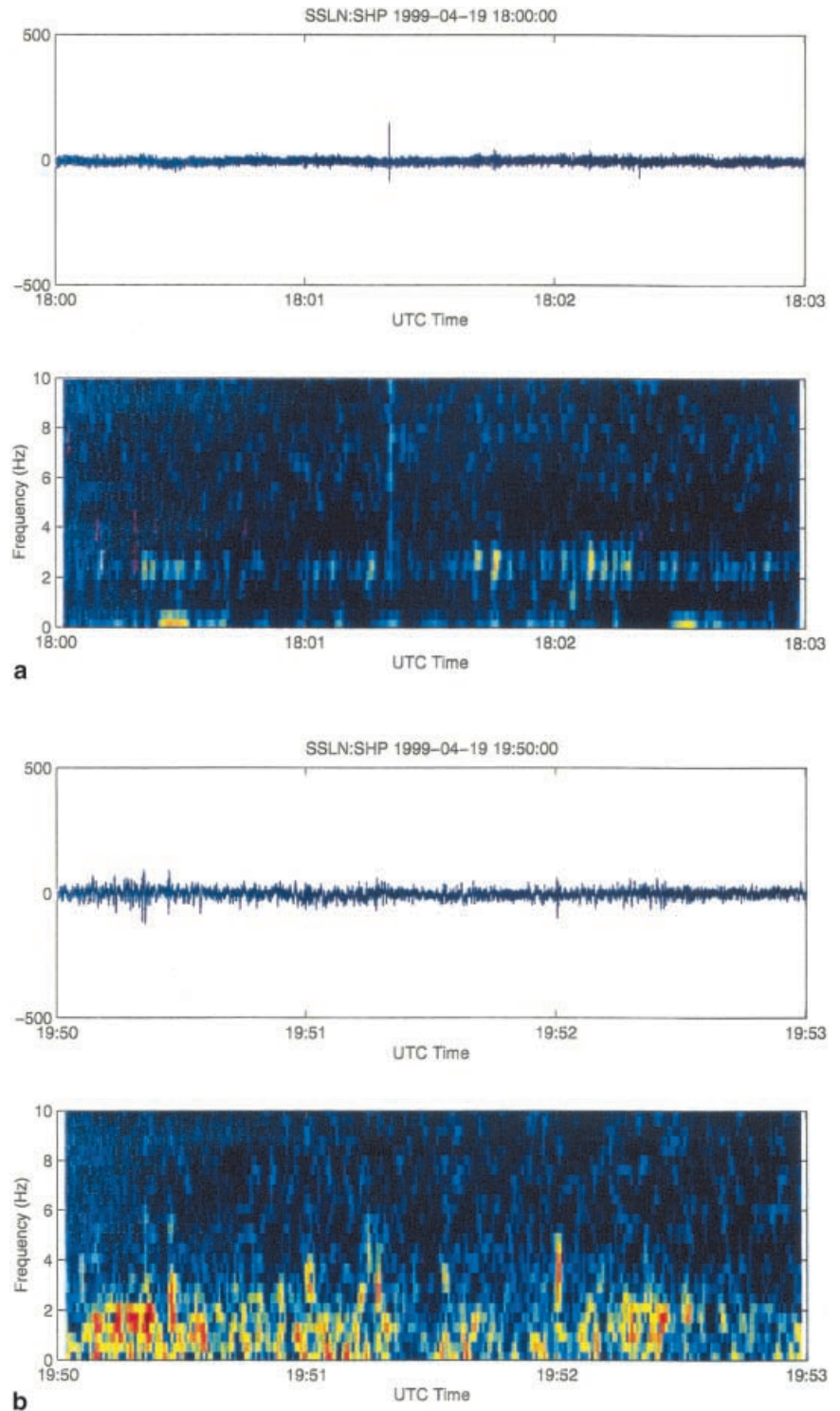
broad-band with the maximum spectral ratio occurring at ~6 Hz, and significant energy between 3.5 and 8.4 Hz. This was determined by measuring the frequency bandwidth at 50% of the amplitude of the maximum peak in Fig. 7b.

The pressure sensor data provided key information to resolve the differences in the tremor. Selected data from each of the eruption phases described above were analyzed by producing standard size time series plots and spectrograms (Fig. 8, Table 1). Explosions could be recognized as distinct pulses in the time series corresponding to ~1 Hz pulses in the spectrograms. We found no explosions strong enough to be recognized during the Strombolian activity on 19 April. No explosions occurred during most of the sub-Plinian phase, with a few recorded near the end (Table 1). When the tremor frequency dropped and the amplitude increased after the sub-Plinian phase, in every case explosions

**Fig. 8a–f** (continued)



SSLN:SHP 1999–04–19 23:05:00



c



SSLN:SHP 1999–04–20 01:00:00



d
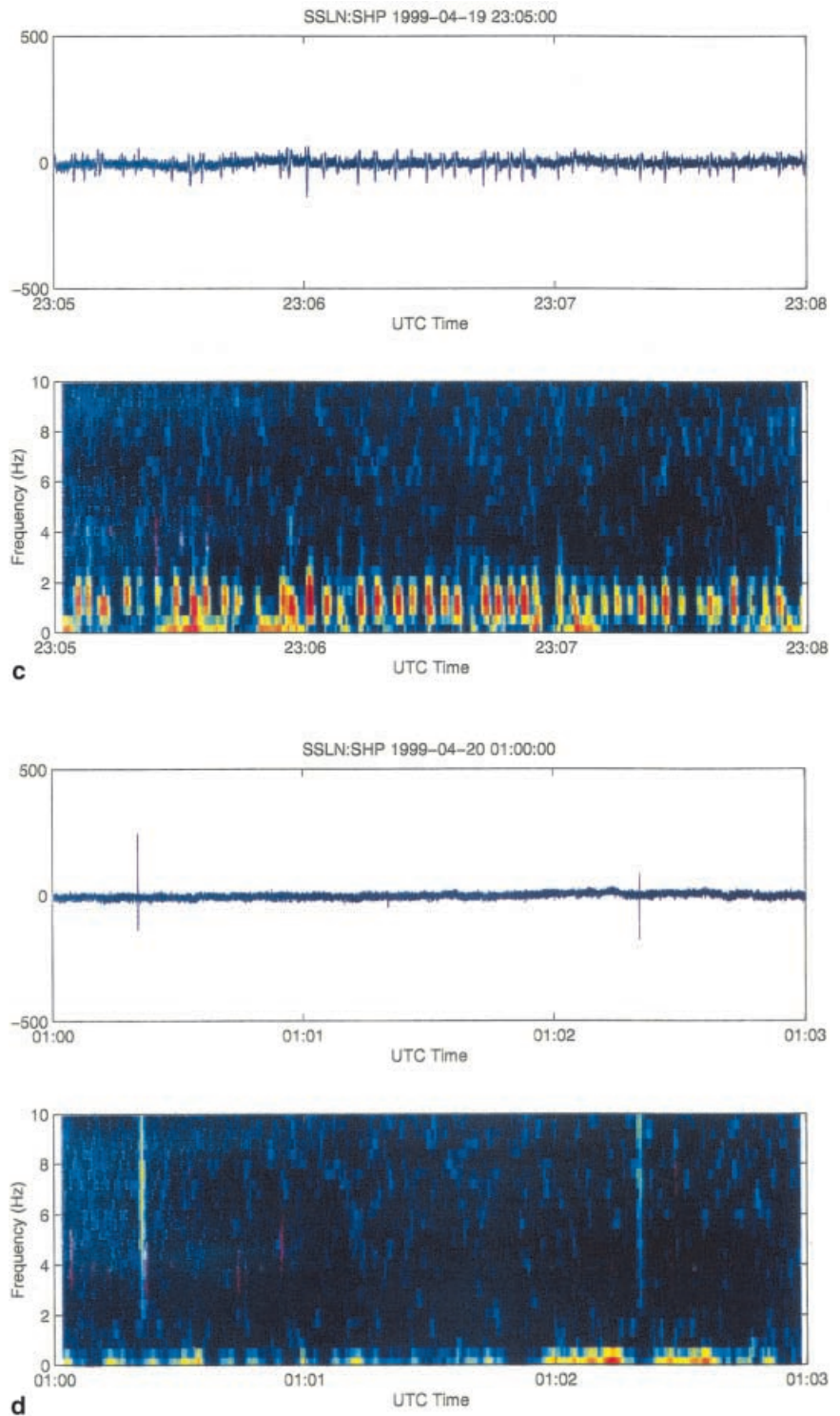
occurred at high rates of 23 to 48 per 3 min (the window length in Fig. 8), and with high amplitudes (Table 1). When the explosions stopped, the tremor frequency returned to 1.3 Hz and the $D_R$ declined. On 23 April, explosions occurred at a rate of 30 per 3 min, and pressure amplitudes were nearly an order of magnitude higher than on 19 April (Table 1). This provides an explanation for the strong volcanic tremor observed on 23 April, but accompanied by only a small plume to 6 km; vigorous Strombolian explosions were occurring every 6 s, but the local seismic data were all saturated so the airwaves could not be seen. In all cases the explosions produced significant energy at and below 1 Hz, both seismically and acoustically (Fig. 8 spectrograms), providing an explanation for the frequency reduction seen in the seismic data (Figs. 4, 5, 6, and 7).

Fig. 8a–f (continued)



SSLN:SHP 1999-04-20 01:47:00



e



SSLN:SHP 1999-04-23 10:01:20



f
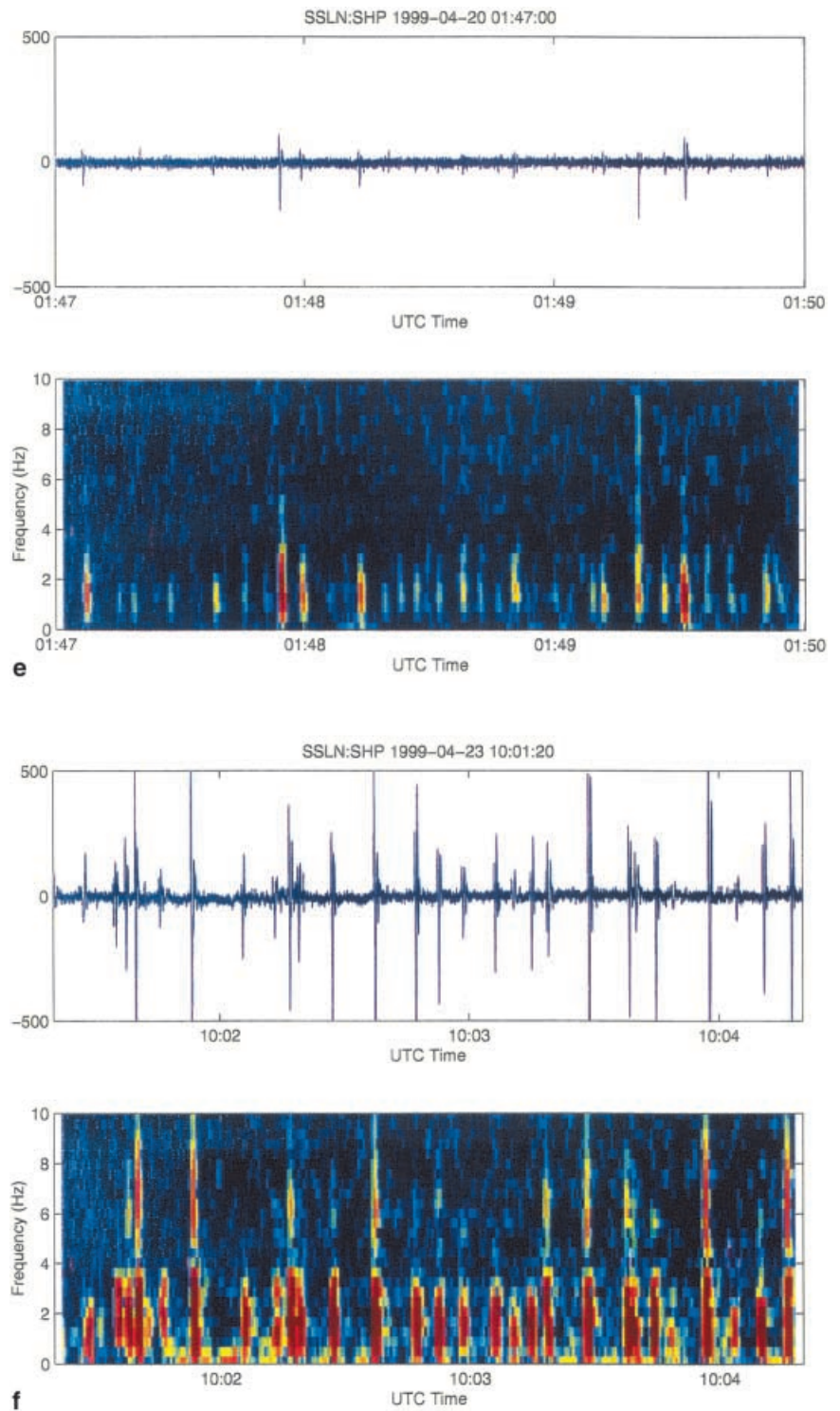
## Discussion

The existence of three distinct tremor spectra and their systematic relation to $D_R$ suggests there may be three distinct tremor source mechanisms. This was confirmed by systematic differences of explosions in pressure data. We infer that these correspond to different flow regimes such as slug flow (Strombolian activity), sustained strong explosions with fracturing of vent fill (sub-Plinian phase), and gas-rich bubbly flow (vigorous Strombolian activity 19 and 23 April). The transition from one flow or eruption regime to another may be caused by variations in gas flux, magma ascent rate, viscosity, or other parameters (e.g., Jaupart and Vergniolle 1988; Parfitt and Wilson 1995). Unfortunately, there is no record of how any of these parameters varied during the course of the

eruption. The tephra from the eruption formed a single deposit with no discernible internal structure or variations in clasts (Stelling et al. 2002, this volume).

These tremor signals could also be interpreted in terms of a resonator model. Transition from high frequency to low frequency tremor could be caused by either an increase in the resonant length of the conduit or a decrease in the sound speed of the fluid in the conduit. Although the sub-Plinian eruption may have modified the near-surface conduit geometry (we consider it to be a "vent-clearing phase," lasting only 80 min, but producing nearly all the erupted volume), this could only account for a single change in tremor frequency and would be a non-repeatable source. However, a change in the resonant length of the conduit does not necessarily imply a change in conduit geometry. In order for resonance to occur, pressure waves must be reflected at some upper and some lower boundary. If the upper boundary is assumed to be the vent, the lower boundary could move. This lower boundary might reflect a sharp transition in fluid properties, such as a bubble nucleation front.

The spectra from the 19 April sub-Plinian phase resemble spectra from earthquakes in that they are relatively rich in higher frequencies (3.5–8.4 Hz). We speculate that extensive fracturing of the conduit fill material may have occurred. Under this scenario it is appropriate to consider the volume change associated with seismic moment release as postulated by McGarr (1976). To do this we computed the total seismic moment for the 80-min eruption using the relation given by Fehler (1983). This yielded a value of $15.3 \times 10^{11}$ N-m. Using the $M_o$ to volume relation of McGarr (1976) gives a volume of $13.3 \times 10^6$ m$^3$, which is within about 10% of the volume of the deposit ($14 \times 10^6$ m$^3$; Stelling et al. 2002, this volume). This calculation does not prove that fracturing occurred, but the close agreement with the theoretical result helps to establish plausibility. McGarr's relation has previously been used to estimate cumulative $M_o$ for earthquakes associated with caldera collapse at Fernandina (McGarr 1976) and Katmai (Abe 1992) with good agreement. It has not previously been used for tremor. We use it here because of the spectral similarities of the sub-Plinian tremor with earthquakes, and recognize that it may not be appropriate to use this formulation for all tremor.

An additional possibility would be a change in the velocity of the magma/gas mixture within the conduit. A decrease in sound speed would occur if the volume density of bubbles in the conduit increased (Kieffer 1977). This implies that during high-amplitude tremor bands, the volume density of bubbles is higher than during bands of low-amplitude tremor. This could either be because of decompression or a higher gas content. The large explosions present in the pressure data strongly suggest that this is indeed the reason for the lowering of frequencies observed in tremor during the strong phases following the sub-Plinian phase on 19 April. The pressure data show the same low frequencies as the tremor. The pressure data are not contaminated by path effects that modify the seismic tremor, but instead are a more di-

rect measure of magmatic conditions at the vent. The seismic and pressure data together provide a consistent picture of some features of the eruptive processes, as has been observed elsewhere (Garcés et al. 1998)

## Conclusions

Volcanic tremor at Shishaldin was stationary from its first appearance in January 1999, through an inferred small Strombolian eruption 7 April, and up to 10:00 h UTC (02:00 h AST) on 19 April 1999. Tremor signals recorded in the hours prior to and immediately after a sub-Plinian eruption at Shishaldin on 19 April 1999, show completely different patterns of behavior. Prior to this event, tremor with a constant spectrum gradually increased in amplitude, and was observed to accompany Strombolian eruptive activity. After the 19 April event, alternating bands of high-amplitude tremor and low-amplitude tremor occurred. Further analysis of these alternating bands shows that dramatic changes in tremor frequency occurred at the same times. Tremor reduced displacements below ~8 cm$^2$ correspond to a peak at 1.3 Hz. Tremor amplitudes above ~ 15 cm$^2$ correspond to a peak at 1.0 Hz. The systematic changes in both amplitude and frequency coincided with the occurrence of strong explosions as indicated by pressure data. This pattern of seismicity did not occur at any other time at Shishaldin, nor has it been noted at any other volcanoes known to us.

These tremor signals are intriguing as they may reflect changes in eruptive style and flow regime within the conduit. Further analyses of seismic and pressure sensor data from the 19 April sequence may elucidate the relationship between tremor amplitude and flow regime/eruptive activity and provide valuable information about how the transition from Strombolian to sub-Plinian activity occurs. We also intend to study the geometry of the magmatic system, and whether or how it was modified during the sub-Plinian eruption on 19 April 1999.

## Appendix

Calculation of reduced displacement

Reduced displacement (DR) is a normalized measure of the amplitude of volcanic tremor, designed so that it can be compared from one volcano to another. Normalization is performed by multiplying the root-mean-square displacement seismogram by a geometrical spreading correction factor. For body waves (spherical wave-

fronts), the geometrical spreading correction factor is r (Aki and Koyanagi 1981), where r= distance from source to seismic station. For surface waves (circular wavefronts), the geometrical spreading correction factor is $\sqrt{\lambda r}$ (Fehler 1983) where l= wavelength.

In order to compute DR from digital data, we took 10.24 s windows of the continuous data, and for each window we calculated a displacement spectrum (with spectral resolution of 0.1 Hz) by fast Fourier transform. We then multiplied this by a geometrical spreading correction factor, to obtain an estimate of the reduced displacement spectrum. We then isolated the tremor signal by choosing the maximum spectral peak between 0.8 and 10 Hz as our volcanic tremor DR. At Shishaldin, the evidence for surface waves versus body waves was inconclusive (both appear to be present), so we chose the surface wave formulation as a default for plots. However, we also calculated the body wave values, and then averaged the results to give preferred values (see Table 2). For body and surface waves we assumed speeds of 4 and 2 km/s, respectively. The depth of the tremor source was assumed to be shallow (<2 km).

The formulations for DR are valid only for a point source recorded in the far field and attenuation and site effects are ignored. Near field effects dominate at distances less than 1 wavelength from the source, and result in faster decay of amplitude than predicted by geometrical spreading. The stations used in this study were 10–17 km from the source. For a peak tremor frequency of 1 Hz, this implies that stations were at least 2.5 wavelengths from the source for body waves, and 5 wavelengths for surface waves. Hence near field effects are likely to be negligible for surface waves, and have only a small effect on body waves.

Attenuation is not included in DR calculations, which is permissible because station distances at many volcanoes are similar (about 5–15 km), thus providing a consistent basis for comparison. However, attenuation is a well known effect and can be estimated from exp(–prf/Qc; e.g., Del Pezzo et al. 1989). We did not calculate Q from our data, but based on other studies (McNutt 1986; Del Pezzo et al. 1989), a surface wave Q of 50, and a body wave Q of 300 seem reasonable. Hence at a distance of 17 km, a surface wave would be attenuated by 1–exp(–p.17.1/50.2)=41%, and a body wave by 1–exp(–p.17.1/300.4)=4.%. When surface wave and body wave DR are averaged, the result would be an under correction by about 20%, which is well within the uncertainty due to site effects. In any case, Q is very poorly constrained, so we feel it would be inappropriate to apply a correction for attenuation to our data. Its neglect does not affect any of the conclusions of this paper.

# References

Abe K (1992) Seismicity of the caldera-making eruption of Mount Katmai, Alaska in 1912. Bull Seismol Soc Am 82:175–191

Aki K, Koyanagi RY (1981) Deep volcanic tremor and magma ascent mechanism under Kilauea, Hawaii. J Geophys Res 86:7095–7110

Benoit JP, Thompson G, Lindquist K, Hansen R, McNutt SR (1998) Near-real-time WWW-based monitoring of Alaskan volcanoes: the IceWeb system. EOS Transactions, AGU 1998 Fall Meeting, vol 79, no 45

Dehn J, Dean KG, Engle K, Izbekov P (2002) Thermal precursors in satellite imagery of the 1999 eruption of Shishaldin Volcano. Bull Volcanol (in press). DOI 10.1007/s00445-002-0227-0

Del Pezzo E, Lombardo G, Spampinato S (1989) Attenuation of volcanic tremor at Mt. Etna, Sicily. Bull Seismol Soc Am 79:1989–1994

Fehler M (1983) Observations of volcanic tremor at Mount St. Helens volcano. J Geophys Res 88:3476–3484

Garcés MA, Hagerty MT, Schwartz SY (1998) Magma acoustics and time-varying melt properties at Arenal Volcano, Costa Rica. Geophys Res Lett 25:2293–2296

Jaupart C, Vergniolle S (1988) Laboratory models of Hawaiian and Strombolian eruptions. Nature 331:58–60

Kieffer SW (1977) Sound speed in liquid–gas mixtures: water–air and water–steam. J Geophys Res 80:2895–2904

McGarr A (1976) Seismic moments and volume changes. J Geophys Res 81:1487–1494

McNutt SR (1986) Observation and analysis of B-type earthquakes, explosions and volcanic tremor at Pavlof Volcano, Alaska. Bull Seismol Soc Am 76:153–175

McNutt SR (1994a) Volcanic tremor amplitude correlated with Volcanic Explosivity Index and its potential use in determining ash hazards to aviation. Acta Vulcanol 5:193–196

McNutt SR (1994b) Volcanic tremor from around the world: 1992 update. Acta Vulcanol 5:197–200

Miller TP, McGimsey RG, Richter DH, Riehle JR, Nye CJ, Yount ME, Dumoulin JA (1998) Catalog of the historically active volcanoes of Alaska. US Geol Surv Open-File Rep 98-582

Moran SC, Stihler SD, Power JA (2002) A tectonic earthquake sequence preceding the April–May 1999 eruption of Shishaldin Volcano, Alaska. Bull Volcanol (in press). DOI 10.1007/s00445-002-0226-1

Nye CJ, Keith TEC, Eichelberger JC, Miller TP, McNutt SR, Moran SC, Schneider DJ, Dehn J, Schaefer J (2002) The 1999 eruption of Shishaldin Volcano, Alaska: monitoring a distant eruption. Bull Volcanol (in press). DOI 10.1007/s00445-002-0225-2

Parfitt EA, Wilson L (1995) Explosive volcanic eruptions – IX: the transitions between Hawaiian-style lava fountaining and Strombolian explosive activity. Geophys J Int 121:226–232

Schneider DJ, Moran SC, Nye CJ (1999) Volcanic clouds from the 1999 eruption of Shishaldin Volcano, Alaska: comparisons of satellite, seismic, and geologic observations. EOS Trans Am Geophys Union 80(Suppl):F1146–F1147

Stelling P, Beget J, Nye C, Gardner J, Devine JD, George RMM (2002) Geology and petrology of ejecta from the 1999 eruption of Shishaldin Volcano, Alaska. Bull Volcanol (in press). DOI 10.1007/s00445-002-0229-y